Journal of Visualized Experiments

Combined in vivo optical and µCT imaging to monitor infection, inflammation and bone anatomy in an orthopaedic implant infection in mice

--Manuscript Draft--

Manuscript Number:	JoVE51612R5
Full Title:	Combined in vivo optical and µCT imaging to monitor infection, inflammation and bone anatomy in an orthopaedic implant infection in mice
Article Type:	Methods Article - JoVE Produced Video
Keywords:	imaging; optical; CT; bioluminescence; fluorescence; staphylococcus; infection; inflammation; bone; orthopaedic; implant; biofilm
Manuscript Classifications:	1.2: Musculoskeletal System; 2.3: Bacteria; 3.1: Bacterial Infections and Mycoses; 3.5: Musculoskeletal Diseases; 5.4: Surgical Procedures, Operative; 5.5: Investigative Techniques; 93.35: Instrumentation and Photography
Corresponding Author:	Lloyd S Miller, M.D., Ph.D. Johns Hopkins University School of Medicine Baltimore, MD UNITED STATES
Corresponding Author Secondary Information:	
Corresponding Author E-Mail:	lloydmiller@jhmi.edu
Corresponding Author's Institution:	Johns Hopkins University School of Medicine
Corresponding Author's Secondary Institution:	
First Author:	Nicholas M Bernthal
First Author Secondary Information:	
Other Authors:	Nicholas M Bernthal
	Brad N Taylor
	Jeffrey A Meganck
	Yu Wang
	Jonathan H Shahbazian
	Jared A Niska
	Kevin P Francis
Order of Authors Secondary Information:	
Abstract:	Multimodality imaging has emerged as a common technological approach used in both preclinical and clinical research. Advanced techniques in combined in vivo optical and µCT imaging allow the visualization of biological phenomena in an anatomical context. These imaging modalities may be especially useful to study conditions that impact bone. In particular, orthopaedic implant infections represent one of the most serious complications in orthopaedic surgery and involve bacterial biofilms that form on the implanted foreign materials, chronic inflammation, osteomyelitis and periprosthetic osteolysis, leading to implant loosening and failure. In this study, a mouse model of an orthopaedic implant infection was used that involved the surgical placement of a Kirschner-wire implant into an intramedullary canal in the femur in such a way that the end of the implant extended into the knee joint. In this model, LysEGFP mice were employed, which have EGFP-fluorescent neutrophils, in conjunction with a bioluminescent strain of Staphylococcus aureus, which was inoculated in the knee joints prior to closing the surgical site. In vivo bioluminescent and fluorescent imaging

	was used to quantify the bacterial burden and neutrophil inflammatory response, respectively. In addition, μCT imaging was performed on the same mice so that the 3D anatomical location of the optical signals could be co-registered with the μCT images using a diffuse optical tomography reconstruction algorithm. To quantify the changes in the bone over time, the outer bone volume of the distal femurs were measured at specific time points using a semi-automated contour based segmentation process. Taken together, the combination of in vivo bioluminescent/fluorescent imaging with μCT imaging may be especially useful for the noninvasive monitoring of the infection, inflammatory response and anatomical changes in bone over time.
Author Comments:	Please note the 2 sites of filming: (1) Johns Hopkins University School of Medicine Department of Dermatology 1550 Orleans Street Cancer Research Building II, Suites 209/210 Baltimore, MD 21231 (2) PerkinElmer 68 Elm Street Hopkinton, MA 01748 More details to come about the exact building/room/location at the Caliper/Perkin Elmer site.
Additional Information:	
Question	**Response**

Cover Letter

Johns Hopkins Department of Dermatology
Cancer Research Building II, Suites 209 & 210
1550 Orleans Street
Baltimore, MD 21231
410-955-8662 T
410-955-8645 F

JOHNS HOPKINS
MEDICINE

August 31, 2013

To Matthew Kramer and the Editors of the *Journal of Visualized Experiments*

We are pleased to submit this manuscript titled "Combined *in vivo* optical and µCT imaging to monitor infection, inflammation and bone anatomy in an orthopaedic implant infection in mice " to the *Journal of Visualized Experiments*.

Multimodality imaging, especially combining *in vivo* optical and µCT imaging, has emerged as a common technological approach used in both preclinical and clinical research. Here, we present a detailed protocol using state-of-the-art *in vivo* optical and µCT imaging to study an orthopaedic implant infection in mice. We demonstrate that these imaging modalities can be combined to noninvasively and longitudinally monitor the dynamics of the bacterial infection, inflammatory response and anatomical changes in the bone. The protocols for the multimodality *in vivo* imaging in this manuscript can be expanded beyond infectious diseases and used across disciplines, including orthopaedics, rheumatology and oncology, to investigate other conditions that impact the musculoskeletal system, such as skeletal cancer, metastatic disease, fractures and arthritis. Thus, we believe this work will be an excellent addition to JoVE's unique multimedia format.

The authors have all made significant contributions to the manuscript: bacterial preparation (Y.W., J.H.S.), mouse surgical procedures (N.M.B., J.A.N., Y.W., J.H.S.), in vivo optical imaging (J.A.M., K.P.F. and L.S.M.), in vivo µCT imaging (J.A.M., K.P.F. and L.S.M.). N.M.B., J.A.M., K.P.F., and L.S.M. designed experiments and helped write the manuscript.

We recommend the following reviewers:

1. Elena Dubikovskaya, Ph.D., École Polytechnique Fédérale de Lausanne, elena.dubikovskaya@epfl.ch
2. Jagath Kadurugamuwa, Ph.D., Alcon Laboratories, Inc., Jagath.Kadurugamuwa@alconlabs.com
3. Philip Hill, Ph.D., University of Nottingham, phil.hill@nottingham.ac.uk
4. Gooitzen van Dam, M.D., Ph.D., University Medical Center Groningen, g.m.van.dam@umcg.nl
5. C. Henrique Serezani, Ph.D., Indiana University, hserezan@iupui.edu
6. Tianhong Dai, Ph.D., Massachusetts General Hospital, tdai@mgh.harvard.edu

Sincerely,

Lloyd S. Miller, M.D., Ph.D.
Associate Professor

TITLE: Combined *in vivo* optical and µCT imaging to monitor infection, inflammation and bone anatomy in an orthopaedic implant infection in mice

AUTHORS:

Nicholas M. Bernthal, Brad N. Taylor, Jeffrey A. Meganck, Yu Wang, Jonathan H. Shahbazian, Jared A. Niska, Kevin P. Francis and Lloyd S. Miller.

1. Bernthal, Nicholas M.
   Department: Orthopaedic Hospital Research Center, Orthopaedic Hospital Department of Orthopaedic Surgery
   Institution: David Geffen School of Medicine at University of California, Los Angeles (UCLA)
   City, Country: Los Angeles, California 90095, USA.
   Email: nbernthal@mednet.ucla.edu

2. Taylor, Brad N.
   Department/Institution: PerkinElmer
   City, Country: Hopkinton, MA, 01748, USA.
   Email: Brad.Taylor@perkinelmer.com

3. Meganck, Jeffrey A.
   Department/Institution: PerkinElmer
   City, Country: Hopkinton, MA, 01748, USA.
   Email: jeffrey.meganck@perkinelmer.com

4. Wang, Yu
   Department: Department of Dermatology
   Institution: Johns Hopkins University School of Medicine
   City, Country: Baltimore, MD 21231, USA.
   Email: ywang107@jhmi.edu

5. Shahbazian, Jonathan H.
   Department: Department of Dermatology
   Institution: Johns Hopkins University School of Medicine
   City, Country: Baltimore, MD 21231, USA.
   Email: jshahba1@jhmi.edu

6. Niska, Jared, A.
   Department: Orthopaedic Hospital Research Center, Orthopaedic Hospital Department of Orthopaedic Surgery
   Institution: David Geffen School of Medicine at University of California, Los Angeles (UCLA)
   City, Country: Los Angeles, California 90095, USA.
   Email: jniska@mendet.ucla.edu

7. Francis, Kevin P.
Department/Institution: PerkinElmer
City, Country: Hopkinton, MA, 01748, USA.
Email: kevin.francis@perkinelmer.com

8. Miller, Lloyd S.
Department: Department of Dermatology
Institution: Johns Hopkins University School of Medicine
City, Country: Baltimore, MD 21231, USA.
Email: lloydmiller@jhmi.edu

CORRESPONDING AUTHOR:
Miller, Lloyd S.
Department: Department of Dermatology
Institution: Johns Hopkins University School of Medicine
City, Country: Baltimore, MD 21231, USA.
Email: lloydmiller@jhmi.edu
Phone: (410) 955-8662
Fax: (410) 955-8645

KEYWORDS:
Imaging, optical, CT, bioluminescence, fluorescence, staphylococcus, infection, inflammation, bone, orthopaedic, implant, biofilm

SHORT ABSTRACT:
Combined optical and μCT imaging in a mouse model of orthopaedic implant infection, utilizing a bioluminescent engineered strain of *Staphylococcus aureus,* provided the capability to noninvasively and longitudinally monitor the dynamics of the bacterial infection, as well as the corresponding inflammatory response and anatomical changes in the bone.

LONG ABSTRACT:
Multimodality imaging has emerged as a common technological approach used in both preclinical and clinical research. Advanced techniques that combine *in vivo* optical and μCT imaging allow the visualization of biological phenomena in an anatomical context. These imaging modalities may be especially useful to study conditions that impact bone. In particular, orthopaedic implant infections are an important problem in clinical orthopaedic surgery. These infections are difficult to treat because bacterial biofilms form on the foreign surgically implanted material, which leads to persistent inflammation, osteomyelitis and eventual osteolysis of the bone surrounding the implant, which ultimately results in implant loosening and failure. Here, a mouse model of an infected orthopaedic prosthetic implant was used that involved the surgical placement of a Kirschner-wire implant into an intramedullary canal in the femur in such a way that the end of the implant extended into the knee joint. In this model, LysEGFP mice, a mouse strain that has EGFP-fluorescent neutrophils, were employed in conjunction with a bioluminescent *Staphylococcus aureus* strain, which naturally emits light. The bacteria were inoculated into the knee joints of the mice prior to closing the surgical site. *In vivo* bioluminescent and fluorescent imaging was used to quantify the bacterial burden and neutrophil

inflammatory response, respectively. In addition, μCT imaging was performed on the same mice so that the 3D location of the bioluminescent and fluorescent optical signals could be co-registered with the anatomical μCT images. To quantify the changes in the bone over time, the outer bone volume of the distal femurs were measured at specific time points using a semi-automated contour based segmentation process. Taken together, the combination of *in vivo* bioluminescent/fluorescent imaging with μCT imaging may be especially useful for the noninvasive monitoring of the infection, inflammatory response and anatomical changes in bone over time.

INTRODUCTION:

Multimodality preclinical imaging techniques that involve the combination of optical and anatomical information allow the visualization and monitoring of biologic phenomena in 3D [1-4]. Since μCT imaging permits the exquisite visualization of bone anatomy, using μCT imaging in conjunction of with optical imaging represents a unique combination that might be especially useful for investigating processes that involve bone biology [5-7]. An example would be to use these techniques to study orthopaedic implant infections, which represent a disastrous complication following orthopaedic surgical procedures [8, 9]. Bacteria biofilms form on the implanted foreign objects that promote survival of the bacteria by serving as a physical barrier that prevents immune cells from sensing the infection and blocks antibiotics from accessing the bacteria [10, 11]. The chronic and persistent infection of the joint tissue (septic arthritis) and bone (osteomyelitis) induces bone resorption that leads to loosening of the prosthesis and eventual failure [8, 9]. This resulting periprosthetic osteolysis is associated with increased morbidity and mortality [12, 13].

In our prior work, *in vivo* bioluminescent and fluorescent imaging was used together with X-ray and micro-computed tomography imaging (μCT) in an orthopaedic prosthetic joint infection model in mice [14-19]. This model involved placing a titanium Kirschner-wire (K-wire) in such a manner that the cut end of the implant extended in the knee joint from the femurs of mice [14-19]. An inoculum of *Staphylococcus aureus* (bioluminescent strain Xen29 or Xen36) was then pipetted onto the surface of the implant in the knee joint before the surgical site was closed [14-19]. *In vivo* optical imaging was used to detect and quantify the bioluminescent signals, which corresponded to the number of bacteria in the infected joint and bone tissue [14-19]. In addition, *in vivo* fluorescence imaging of LysEGFP mice, which possess fluorescent neutrophils [20], was used to quantify the numbers of neutrophils that emigrated to the infected knee joints containing the K-wire implants [14, 19]. Finally, anatomical imaging modalities, including high-resolution X-ray imaging and μCT imaging, permitted respective 2D and 3D anatomic imaging of the affected bone over the entire duration of chronic infection, which we would arbitrarily end typically between 2 and 6 postoperative weeks [16, 18]. Using this model, the efficacy of local and systemic antimicrobial therapy, protective immune responses and pathologic anatomical changes in bone could be evaluated [14-18]. In this manuscript, the detailed protocols for the optical and μCT imaging modalities in this orthopaedic prosthetic joint infection model were provided as a representative system to study biological processes in the anatomic context of the bone. These include the surgical procedures to model an orthopaedic prosthetic joint infection in mice, 2D and 3D *in vivo* optical imaging procedures (to detect bacterial bioluminescent signals and fluorescent neutrophil signals), μCT imaging acquisition and analysis and co-registration of 3D optical images with the μCT images.

PROTOCOL:

Ethics statement: All animals were handled in strict accordance with good animal practice as defined in the federal regulations as set forth in the Animal Welfare Act (AWA), the 1996 Guide for the Care and Use of Laboratory Animals and the PHS Policy for the Humane Care and Use of Laboratory Animals and all animal work was approved by the Johns Hopkins Animal Care and Use Committee (Protocol #: MO12M465).

1) Preparing the inoculum of mid-logarithmic bioluminescent bacteria

1.1) Streak bioluminescent *S. aureus* strain Xen36 onto tryptic soy agar plates (tryptic soy broth in agar [1.5%]). Note: *S. aureus* Xen36[21] is a genetically engineered *S. aureus* strain that contains a modified *lux* operon derived from *Photorhabdus luminescens*, which is integrated into a stable native plasmid found in this bacterial strain. These engineered bacteria constitutively emit light from live and metabolically active cells.

1.2) Grow the colonies on the plates by incubating them at 37°C for approximately 16 hours (overnight).

1.3) Select single bacterial CFU and culture in shaking liquid TSB (240 rpm) for approximately 16 hours (overnight).

1.4) Perform a sub-culture with 1/50 dilution of the overnight culture to obtain mid-logarithmic growth phase bacteria (approximately 2 hour duration).

1.5) Pellet, resuspend and wash the bacteria 3 times in PBS.

1.6) Estimate the bacterial inocula ($1x10^3$ CFU in 2 µl PBS) by determining the optical density absorbance at 600 nm.

1.7) Verify the CFU in the inoculum after culturing the bacteria overnight on plates.

2) Mouse surgical procedures

Note: For these experiment, use a twelve-week old male LysEGFP mice. These mice possess enhanced green fluorescent protein (EGFP) expressing myeloid cells (which consist of mostly neutrophils) [20]. Maintain sterile conditions during surgery and after surgical prep with betadine and 70% alcohol by placing each mouse on a sterile drape on top of a hard surface water circulating heating pad. Use gown, sterile gloves, mask and sterilize instruments.

2.1) Anesthetize the mouse using a 2% inhalation of isoflurane. Use vet ointment on eyes to prevent dryness while under anesthesia. Assess the appropriate level of anesthesia by observing the respiratory rate, muscle tone, toe pinch, corneal reflex and color of mucous membranes. Cover the mice with a sterile surgical drape with a hole at the surgery site on the right knee.

2.2) Inject buprenorphine (sustained-release formulation) (2.5 mg/kg) subcutaneously just prior to surgery. Additional doses of sustained-release buprenorphine may be administered at 3 day intervals as needed for analgesia.

2.3) Shave the operative knee and prep using three alternating scrubs using betadine and 70% alcohol.

2.4) Perform a midline incision in the skin overlying the right knee joint. Extend the skin incision so that the extensor mechanism can be well defined.

2.5) Perform a medial parapatellar arthrotomy and sublux the quadriceps-patellar tendon extensor mechanism laterally with an Adson forceps. Note: This brings the intercondylar notch of the femur into plain view.

2.6) Manually ream the intramedullary canal using a 25 gauge needle followed by a 23 gauge needle. Note: Care must be taken to remain parallel to the femoral shaft so as to avoid asymmetric reaming and potential femur fracture.

2.7) Insert a medical-grade titanium Kirschner-wire (0.8 mm diameter) by using a press-fit technique, which entails manually pushing it using a pin holder, in a retrograde direction into the intramedullary canal. Note: Titanium K-wires were used as there were fewer artifacts seen on the μCT images with titanium K-wires compared with stainless steel K-wires [16].

2.8) Cut the end of the Kirschner-wire with pin cutters so that the cut end of the K-wire extends approximately 1 mm into the knee joint space.

2.9) Using a micropipette, pipette 2 μL of $1x10^3$ CFU of bioluminescent *S. aureus* Xen36 onto the tip of the implant within the knee joint space.
Note: More volume leads to wider tissue contamination and less discrete imaging.
Note: In control uninfected mice, add 2 μL of sterile saline without any bacteria.

2.10) Reduce the quadriceps-patellar complex back to midline using forceps and close the overlying subcutaneous tissue and skin using absorbable subcuticular sutures.

Note: Do not leave an animal unattended until it has regained sufficient consciousness to maintain sternal recumbency. Do not return an animal that has undergone surgery to the company of other animals until fully recovered.

2.11) At the end of the experiments, euthanized all animals using carbon dioxide inhalation according the Johns Hopkins Animal Care and Use Committee guidelines. Verify death by observing the animal fails to recover within 10 minutes after carbon dioxide exposure ends and cervical dislocation.

3) 2D optical imaging (*in vivo* bioluminescent and fluorescent imaging).

3.1) Anesthetize LysEGFP mice (e.g., 2% inhalation isoflurane) and place them with ventral side up into an imaging chamber.

3.2) Perform *in vivo* bioluminescent imaging using the IVIS Spectrum optical whole animal *in vivo* imaging system. First, check Luminescent and confirm the choice of an open filter selection, field of view (FOV) C -13 cm, and scroll exposure time down to Auto (autoexposure setting). Autoexposure will automatically adjust acquisition time (shutter speed), binning (digital pixel binning), and f-stop (aperture) of the instrument to optimize signal intensity while avoiding saturation. Then click Acquire to capture the bioluminescent image.

Note: For *in vivo* bioluminescent imaging, image mice between 1 to 5 minutes.

3.3) Perform sequential *in vivo* fluorescent imaging by checking the box next to Fluorescent. Choose the 465 nm excitation filter and 520 nm emission filter. Scroll exposure time down to Auto and select FOV C (Step 3.2.1). Then click Acquire to capture the fluorescence image.

Note: For *in vivo* fluorescent imaging, image mice between 0.5 seconds.

3.4) Quantify the *in vivo* bioluminescent signals as total flux (photons/s) in a region of interest (ROI) using Living Image software by first expanding the ROI Tools section of the Tool Palette.

3.4.1) Select the Circle Icon and the number of ROIs which correspond to the number of subject animals in the FOV. Resize the ROI to encompass the region of interest i.e. the bioluminescent diffusion pattern collected.

3.4.2) Select Measure ROIs in ROI Tools in the Tool Palette and the ROI Measurement Window will appear. Total Radiance (photons/sec) values represent the sum of bioluminescent pixels within the generated ROI.

3.4.3) Select All and Copy tabs in the bottom right hand corner of this window will transfer the information to the clipboard and allow pasting into subsequent programs for analysis.

3.5) Quantify the *in vivo* fluorescent signals as total radiant efficiency ([photons/s] / [µW/cm²]) within a circular region of interest (ROI) using Living Image software.

3.5.1) Within the Living Image software window, expand ROI Tools in the Tool Palette. Select the Circle Icon and the number of ROIs which corresponds to the number of subject animals in the FOV.

3.5.2) Resize the ROI to encompass the region of interest corresponding closely to the bioluminescent signal from the previous image acquisition.

3.5.3) Select Measure ROIs in ROI Tools in the Tool Palette and the ROI Measurement Window will appear. Note: Total Radiant Efficiency ([photons/s] / [µW/cm²]) represents the sums of fluorescent pixels within the ROI.

3.5.4) Select All and Copy tabs in the bottom right hand corner of this window will transfer the information to the clipboard and allow pasting into subsequent programs for analysis.

4) µCT image acquisition

4.1) Place the anesthetized LysEGFP mice into an imaging chamber. Note: This imaging chamber is designed to fit in both the IVIS Spectrum imaging system and the Quantum FX *in vivo* µCT imaging system to allow co-registration of the optical and µCT images.

4.2. Open the CT software and select the Menu preset 60mm FOV std dynamic from the dropdown.

4.3) Insert the large bore cover and the adapter arm for the imaging shuttle into the instrument.

4.4) Place the mouse imaging shuttle into the adapter arm then push the arm into the bore and close the door. Turn on Live Mode (the Eye Button on the Control Panel) and position the subject at the 0 and 90 degree gantry position using the X-axis and Y-axis controls to center the animal in the X capture window. Then turn off Live Mode by clicking the Eye Button.

4.5) Acquire a dynamic scan image with the 60 mm FOV by clicking the CT Scan button (next to the Live Mode Button). Export the acquired image in the DICOM format and store in a location that can be accessed later. Note: The approximate dose will be 26 mGy per scan. A 30 mm FOV can be used if better resolution is desired.

5) 3D optical image acquisition, formation and µCT co-registration.

5.1) Place the mouse imaging shuttle insert into the Spectrum by positioning the imaging shuttle containing the mouse into this insert and ensure the mouse does not move.

5.2) Using Living Image, select Imaging Wizard in the Acquisition Control Panel to begin the wizard setup. To start, choose Bioluminescence>DLIT and then select the reporter "Bacteria" from the dropdown menu and the appropriate emission filters for the model will be chosen automatically, in this case, 500 nm – 620 nm.

5.2.1) Select Next, then designate the acquisition parameters and subject information in the final window. Specifically, Imaging Subject will be Mouse, Auto Settings will be selected allowing autoexposure to maximize signal quality while avoiding saturation, and Field of View will be set to C – 13cm.

5.2.2) Select Finish in the final window and the sequence window of the Acquisition Panel will be automatically populated with the DLIT sequence. There will be one image acquired per emission filter chosen and autoexposure will choose optimal settings at each wavelength as per the Imaging Wizard selections. The generated sequence also includes a structured light image needed for subject surface generation via the Surface Topography tool detailed below.

5.3) Select Acquire Sequence to acquire the DLIT data.

5.4) After the image acquisition is complete, generate the surface topography. Start by expanding the Surface Topography tab under the Tool Palette.

5.4.1) Select the orientation of the animal facing the CCD. Then click Generate Surface. Crop the region of the FOV that contains the animal.

5.4.2) Then use the purple mask to define the bounds of the animal. Note: The masking tool uses color contrast so animals with dark fur or skin will not mask appropriately from the stage.

5.4.3) Select Finish and the surface will appear automatically. Save the result under the Surface Topography tab then close the tab as we will no longer need it.

5.5) Reconstruct the 3D optical source position using the diffuse optical reconstruction algorithms implemented in Living Image[22] by expanding the DLIT 3D Reconstruction tab.

5.5.1) Images acquired for the DLIT sequence are shown. Note: The software automatically verifies quality of the acquired data and will deselect images deemed too dim or where saturation is present. Select Start on the bottom right-hand side.

5.5.2) If required, one can adjust the threshold for each bioluminescent image by double clicking and using the thresholding slider on the bottom left hand side. Note: this is mainly to include lower intensity signal and caution should be practiced when thresholding higher as this may adjust overall intensity of the final reconstructed source.

5.5.3) When satisfied with the threshold, select Reconstruct to automatically run the reconstruction algorithms which will result in a 3D representation of the optical source.

5.6) Open the DICOM browser by clicking the 3D icon in the Tool Bar at the top of the software (third from left) and search for the Quantum FX image acquired previously.

5.6.1) Load this image into the Living Image 3D View tab by double clicking on the file for import. Note: The fiducial should be automatically detected and result in the μCT image being registered with the 3D optical image.

5.7) Deselect the surface topography visualization map by expanding 3D Optical Tools in the Tool Palette and deselecting the check box labeled Display Subject Surface in the Surface tab.

5.8) Manually create a lookup table to visualize the skeleton and the K-wire implant that are visible in the μCT image using the histogram under the Volume tab of the 3D Multi-Modality Tools section of the Tool Palette.

5.8.1) The histogram represents the distribution of voxel intensities in the 3D volumetric data and their color opacity. To determine where the particular tissue of interest is in the histogram, use the slider tool to threshold the rendering until the tissue or structure is visible.

5.8.2) Then right click in the histogram to generate points and form a curve to isolate that area of the histogram. This will be repeated for each structure – skeleton followed by the K-wire implant and can be saved as a lookup table for future analyses.

5.8.3) Components can be color coded if so desired by double clicking any generated point in the histogram and selecting the desired color from the pop up window.

6) µCT image visualization and analysis

6.1) Using the Quantum FX software, select the image of interest and launch Viewer. Select the rotate tool and reorient the image to visualize the longitudinal axis of the femur. Select the measurement tool and measure the femur length.

6.2) Launch the 3D Viewer to generate 3D renderings. Adjust the threshold to show the changes in bone anatomy associated with implant infection.

6.3) Apply clipping planes so that the 3D rendering is limited to the desired cross-sectional section of the area of interest in the distal femur.

6.4) Launch the Analyze 11.0 software package. Load the *.VOX file that was used to create the 3D rendering.

6.5) Launch the Image Calculator tool. Use the 'Region Pad' tool to crop the image (remove planes that don't include the femur).

6.6) Launch the Oblique Sections tool. Use the 3 points option to find points at the middle of the femur, greater trochanter and the end of the pin. Make these points an oblique plane and generate an image with new slices.

6.7) Launch the Region of Interest tool. Display the transaxial slices. Adjust the min and max settings to display the cortical bone. Create contours for the slices corresponding for a several slices (with an approximate interval of 5 slices) for the slices corresponding to the distal 25% of the femur. Use the 'Propagate Regions' tool to interpolate between these contours and create a 3D region of interest. Save this region of interest as an object map.

6.8) Launch the 'Sample Options' tool. Select the checkbox for the object map that was just created and select the radio buttons for the appropriate options. Click the 'Configure Log Stats' button to confirm that the 'Volume' checkbox is selected. Click the 'Sample Images' button to make the actual measurements.

6.9) Export the volume measurements into a data analysis program. Normalize the outer bone volumes from later time points to the first imaged time point using the formula: Δ Volume (%) = ([Volume(day X) – Volume(day 2)]/[Volume(day 2)]) x 100. Note: In this formula, the variable "X" represents the time point of interest. The resultant number will represent the change in the size of outer bone volume of the distal femur over time.

6.10) To visualize the 3D region of interest on top of the bone, load the CT image in the 'Volume Render' tool. Load the object map containing the 3D region of interest. Go to 'View'→'Objects' and set the 'Original' to be 'On'. Open the 'Preview' window. Launch the 'Render Types' menu and select 'Object compositing'.

6.11) Click the 'Threshold' button and tool and adjust the thresholds to show the bone and object map. Use the same fixed threshold range for all time points. Click the 'Rotation' button and set the orientation to be a true anterolateral view. Click 'Render' to generate the final rendering. Save the rendering from the main 'Volume Render' window.

REPRESENTATIVE RESULTS:

***In vivo* bioluminescent and fluorescent imaging**

In the present study, the protocol is described for this previously published model of an orthopaedic prosthetic joint infection in mice [14-19], which involves the surgical placement of a titanium K-wire implant that extends from an intramedullary canal in the femur into the joint space [14-19]. *S. aureus* bioluminescent strain Xen36 ($1x10^3$ CFU in 2 µl PBS) was pipetted directly on top of the end titanium implant in the knee joint prior to closing the surgical site. To visualize and quantify the bacterial burden and neutrophil influx noninvasively in anesthetized LysEGFP mice, *in vivo* whole animal optical imaging was performed to sequentially image the bioluminescent signals from the bacteria and the EGFP fluorescent signals from the infiltrating neutrophils using the IVIS Spectrum optical whole animal *in vivo* imaging system on three postoperative days (i.e., days 2, 14 and 28). The bioluminescent signals of Xen36-infected mice remained above background signals of sham-infected mice for the duration of the experiment (Figure 1A,C). Our previous work demonstrated that the *in vivo* bioluminescent signals closely approximated the numbers of *ex vivo* CFU isolated from the joint/bone tissue and adherent to the implants [17, 18]. In addition, the EGFP fluorescent signals were higher than sham-infected mice at early time points but approached background levels during the course of infection (Figure 2B,C).

3D co-registration of *in vivo* optical signals with µCT images

To visualize the optical signals (i.e., bacterial bioluminescent and EGFP fluorescent signals) in the anatomical context of the post-surgical knee joints in 3D, the optical images generated using the IVIS Spectrum imaging system were co-registered with µCT images generated using the Quantum FX µCT imaging system. This co-registration could be accomplished because the mouse imaging chamber could be inserted into either machine to ensure that the mice were in the exact same orientation. To verify this accuracy, the results were compared with an image acquisition performed using the IVIS Spectrum-CT *in vivo* imaging system that integrates both modalities into one instrument without requiring physical relocation of the animal. To map the optical data onto the µCT images in 3D, we utilized a diffuse optical tomography reconstruction algorithm [16]. The resultant 3D reconstruction is shown (Movie 1).

In addition, µCT imaging allowed the visualization and quantification of the consequential changes in the quality and dimensions of the bone that occurred during the infection (Figure 2). As previously reported, the outer bone volume of the distal femur substantially increased over time (Figure 2A) [16]. To quantify these changes, 3D volumetric image analysis was performed on the distal 25% of the boney surface of the femur and the changes in the bone volume over time were normalized to the initial bone volume. The outer bone volume substantially increased in

infected mice compared to sham-infected mice (Figure 2B). The increase in the distal femur outer bone volume was likely due to bone damage caused by the infection of the joint tissue and bone, which were observed using μCT imaging and histologic analysis [16].

FIGURE LEGENDS:

Figure 1: 2D *in vivo* bioluminescent and fluorescent signals. *S. aureus* Xen36 or no bacteria (uninfected) were inoculated into the knee joint after K-wire placement and LysEGFP mice were imaged using the IVIS Spectrum imaging system. (A) Mean *in vivo* bioluminescent signals as measured by total flux (photons/s) ± sem. (B) Mean *in vivo* EGFP fluorescent signals as measured by total radiant efficiency (photons/s) / (μW/cm²) ± sem. (C) Representative *in vivo* bioluminescent and fluorescent signals overlaid onto a black and white photographic image of the mice. The limit of detection of the bacterial burden using *in vivo* bioluminescent imaging is between $1x10^2$ and $1x10^3$ CFU. *p<0.05, †p<0.01, ‡p<0.001 Xen36-infected mice versus sham-infected mice (Student's t-test [two-tailed]). Please note this is a representative figure that includes previous data generated using Xen29 and imaged with the IVIS Lumina XR imaging system[16]. For this manuscript, we will replace the data in this figure with data using the brighter bioluminescent *S. aureus* strain Xen36 and the IVIS Spectrum imaging system [19].

Figure 2. 3D μCT imaging. *S. aureus* Xen36 or no bacteria (uninfected) were inoculated into the knee joint after K-wire placement and mice were imaged using the Quantum FX *in vivo* μCT system. (A) Representative 3D μCT renderings of Xen36 -infected mice (upper panels) and sham-infected mice (lower panels). (B) Percentage of outer bone volume change (distal 25% of the femurs) normalized to the initial time point (mean ± sem). *p<0.05, †p<0.01, ‡p<0.001 Xen36-infected mice versus sham-infected mice (Student's t-test [two-tailed]). Please note this is a representative figure that includes images generated using the bioluminescent strain *S. aureus* Xen29 [16]. For this manuscript, we will replace the data in this figure with data obtained using the brighter bioluminescent *S. aureus* strain Xen36 [19].

Movie 1. Representative 3D anatomical co-registration of the Xen36 bioluminescent signals and the EGFP-neutrophil fluorescent signals in combination with the μCT images. The images are rotated on the vertical axis. Please note this is a representative figure that includes images generated using the bioluminescent strain *S. aureus* Xen29 [16]. For this manuscript, we will repeat these experiments using the bright bioluminescent *S. aureus* strain Xen36 [19].

DISCUSSION:

Multimodality imaging such as imaging techniques that utilize *in vivo* optical imaging in conjunction with μCT imaging provides a new technological approach that allows the 3D visualization, quantification and longitudinal monitoring of biologic processes in an anatomical context [1-4]. The protocols in the present study provide detailed information of how *in vivo* bioluminescent and fluorescent imaging can be combined with μCT imaging in an orthopaedic prosthetic implant infection model in mice to monitor the bacterial burden, neutrophilic inflammation and anatomical changes in the bone noninvasively and longitudinally over time. Taken together, the information obtained by combining optical and structural imaging represents a major technological advance, which may be particularly well-suited to study biological processes and pathological conditions that affect the musculoskeletal system.

One interesting finding that should be pointed out is that we observed that the EGFP-neutrophil fluorescent signals decreased to background levels by 14-21 days and remained at background levels for the duration of the experiment despite the presence of bioluminescent bacteria. It is unlikely that the X-ray irradiation impacted neutrophil survival as we observed similar kinetics of the neutrophil signals in non-irradiated mice [19]. In our previous work involving a model of *S. aureus* infected wounds, neutrophil infiltration involved a combination of robust neutrophil recruitment from the circulation, prolonged neutrophil survival at the site of infection and the homing of KIT+ progenitor cells to the abscess, where they locally give rise to mature neutrophils[23]. It is likely that similar processes contributed to neutrophil infiltration in the orthopaedic implant *S. aureus* infection model. Although it is unknown why the neutrophil signals decreased in the orthopaedic infection model, it could be that the immune response changed over time as this infection progressed from an acute to chronic infection and this is a subject of future investigation.

There are limitations with this mouse model of orthopaedic prosthetic joint infection and the *in vivo* multimodality imaging that should be noted. First, this mouse model is an oversimplification of the actual procedures and materials used in orthopaedic surgery in humans [24]. Nonetheless, this model does recapitulate the chronic infection and ensuing inflammation in the bone and joint tissue that is seen in human orthopaedic implant infections [8, 9]. In addition, to obtain the μCT images, relatively low doses of X-ray irradiation were used to minimize any adverse effects on the health of the animals during the course of infection. For better resolution of bone, higher doses of X-ray radiation could be used for μCT imaging on euthanized animals. However, this would eliminate the capability to noninvasively and longitudinally monitor the bone changes over the duration of the experiments.

In conclusion, multimodality imaging involving the combination of *in vivo* whole animal optical imaging with anatomical μCT imaging has permitted more comprehensive information about the infection and inflammatory response. In addition, these techniques have permitted the evaluation of the consequences of the infection and inflammation on the bone and joint tissue. Future work could take advantage of multimodality imaging to evaluate the efficacy of antimicrobial therapies, immune responses, pathogenesis of disease and the reactive changes in the bone as we have begun to investigate [14-18]. In addition, multimodality imaging could evaluate probes and tracers to diagnose the presence of an infection as previously described in animal models a thigh infection, endocarditis, pulmonary infections and biomaterial infections[25-28]. Finally, the use of the multimodality imaging could be expanded beyond infectious diseases and used across disciplines, including orthopaedics, rheumatology and oncology, to investigate other conditions that impact the musculoskeletal system, such as skeletal cancer, metastatic disease, fractures and arthritis [5-7].

ACKNOWLEDGMENTS:

This work was supported by an H & H Lee Surgical Resident Research Scholars Program (to J.A.N.), an AO Foundation Start-Up grant S-12-03M (to L.S.M.) and a National Institutes of Health grant R01-AI078910 (to L.S.M.).

DISCLOSURES:
J.A.M., B.N.T., E.L., N.Z., K.P.F. are paid employees of PerkinElmer, which manufactures the imaging instruments, provided the Xen36 bioluminescent *S. aureus* strain and paid for the publication costs. The remaining authors have nothing to disclose.

REFERENCES

1. Dothager, R. S. et al. Advances in bioluminescence imaging of live animal models, *Curr. Opin. Biotechnol.*, **20**, 45-53, DOI: S0958-1669(09)00006-8 [pii];10.1016/j.copbio.2009.01.007 [doi] (2009).
2. Badr, C. E. & Tannous, B. A. Bioluminescence imaging: progress and applications, *Trends Biotechnol.*, **29**, 624-633, DOI: S0167-7799(11)00114-4 [pii];10.1016/j.tibtech.2011.06.010 [doi] (2011).
3. Luker, G. D. & Luker, K. E. Optical imaging: current applications and future directions, *J. Nucl. Med.*, **49**, 1-4, DOI: jnumed.107.045799 [pii];10.2967/jnumed.107.045799 [doi] (2008).
4. Ntziachristos, V., Ripoll, J., Wang, L. V. & Weissleder, R. Looking and listening to light: the evolution of whole-body photonic imaging, *Nat. Biotechnol.*, **23**, 313-320, DOI: nbt1074 [pii];10.1038/nbt1074 [doi] (2005).
5. Reumann, M. K., Weiser, M. C. & Mayer-Kuckuk, P. Musculoskeletal molecular imaging: a comprehensive overview, *Trends Biotechnol.*, **28**, 93-101, DOI: S0167-7799(09)00217-0 [pii];10.1016/j.tibtech.2009.11.004 [doi] (2010).
6. Snoeks, T. J., Khmelinskii, A., Lelieveldt, B. P., Kaijzel, E. L. & Lowik, C. W. Optical advances in skeletal imaging applied to bone metastases, *Bone*, **48**, 106-114, DOI: S8756-3282(10)01396-7 [pii];10.1016/j.bone.2010.07.027 [doi] (2011).
7. Sjollema, J. et al. The potential for bio-optical imaging of biomaterial-associated infection in vivo, *Biomaterials*, **31**, 1984-1995, DOI: S0142-9612(09)01312-X [pii];10.1016/j.biomaterials.2009.11.068 [doi] (2010).
8. Del Pozo, J. L. & Patel, R. Clinical practice. Infection associated with prosthetic joints, *N. Engl. J. Med.*, **361**, 787-794, DOI: 361/8/787 [pii];10.1056/NEJMcp0905029 [doi] (2009).
9. Parvizi, J., Adeli, B., Zmistowski, B., Restrepo, C. & Greenwald, A. S. Management of periprosthetic joint infection: the current knowledge: AAOS exhibit selection, *J. Bone Joint Surg. Am.*, **94**, e104, DOI: 1216215 [pii];10.2106/JBJS.K.01417 [doi] (2012).
10. Arciola, C. R., Campoccia, D., Speziale, P., Montanaro, L. & Costerton, J. W. Biofilm formation in Staphylococcus implant infections. A review of molecular mechanisms and implications for biofilm-resistant materials, *Biomaterials*, **33**, 5967-5982, DOI: S0142-9612(12)00572-8 [pii];10.1016/j.biomaterials.2012.05.031 [doi] (2012).
11. Zimmerli, W. & Moser, C. Pathogenesis and treatment concepts of orthopaedic biofilm infections, *FEMS Immunol. Med. Microbiol.*, **65**, 158-168, DOI: 10.1111/j.1574-695X.2012.00938.x [doi] (2012).

12. Cram, P. et al. Total knee arthroplasty volume, utilization, and outcomes among Medicare beneficiaries, 1991-2010, *JAMA*, **308**, 1227-1236, DOI: 1362022 [pii];10.1001/2012.jama.11153 [doi] (2012).

13. Wolf, B. R., Lu, X., Li, Y., Callaghan, J. J. & Cram, P. Adverse outcomes in hip arthroplasty: long-term trends, *J. Bone Joint Surg. Am.*, **94**, e103, DOI: 1216214 [pii];10.2106/JBJS.K.00011 [doi] (2012).

14. Bernthal, N. M. et al. A mouse model of post-arthroplasty *Staphylococcus aureus* joint infection to evaluate in vivo the efficacy of antimicrobial implant coatings, *PLoS. ONE.*, **5**, e12580, DOI: 10.1371/journal.pone.0012580 [doi] (2010).

15. Bernthal, N. M. et al. Protective role of IL-1beta against post-arthroplasty *Staphylococcus aureus* infection, *J. Orthop. Res.*, **29**, 1621-1626, DOI: 10.1002/jor.21414 [doi] (2011).

16. Niska, J. A. et al. Monitoring bacterial burden, inflammation and bone damage longitudinally using optical and muCT imaging in an orthopaedic implant infection in mice, *PLoS. ONE.*, **7**, e47397, DOI: 10.1371/journal.pone.0047397 [doi];PONE-D-12-17997 [pii] (2012).

17. Niska, J. A. et al. Daptomycin and tigecycline have broader effective dose ranges than vancomycin as prophylaxis against a *Staphylococcus aureus* surgical implant infection in mice, *Antimicrob. Agents Chemother.*, **56**, 2590-2597, DOI: AAC.06291-11 [pii];10.1128/AAC.06291-11 [doi] (2012).

18. Niska, J. A. et al. Vancomycin-Rifampin Combination Therapy has Enhanced Efficacy Against an Experimental *Staphylococcus aureus* Prosthetic Joint Infection, *Antimicrob. Agents Chemother.*, 57, 5080-5086, DOI: AAC.00702-13 [pii];10.1128/AAC.00702-13 [doi] (2013).

19. Pribaz, J. R. et al. Mouse model of chronic post-arthroplasty infection: noninvasive in vivo bioluminescence imaging to monitor bacterial burden for long-term study, *J. Orthop. Res.*, **30**, 335-340, DOI: 10.1002/jor.21519 [doi] (2012).

20. Faust, N., Varas, F., Kelly, L. M., Heck, S. & Graf, T. Insertion of enhanced green fluorescent protein into the lysozyme gene creates mice with green fluorescent granulocytes and macrophages, *Blood*, **96**, 719-726 (2000).

21. Brand, A. M., de, K. M. & Dicks, L. M. The ability of nisin F to control *Staphylococcus aureus* infection in the peritoneal cavity, as studied in mice, *Lett. Appl. Microbiol.*, **51**, 645-649, DOI: 10.1111/j.1472-765X.2010.02948.x [doi] (2010).

22. Kuo, C., Coquoz, O., Troy, T. L., Xu, H. & Rice, B. W. Three-dimensional reconstruction of in vivo bioluminescent sources based on multispectral imaging, *J. Biomed. Opt.*, **12**, 024007, DOI: 10.1117/1.2717898 [doi] (2007).

23. Kim, M. H. et al. Neutrophil survival and c-kit+-progenitor proliferation in *Staphylococcus aureus*-infected skin wounds promote resolution, *Blood*, **117**, 3343-3352, DOI: blood-2010-07-296970 [pii];10.1182/blood-2010-07-296970 [doi] (2011).

24. Deirmengian, C. A. & Lonner, J. H. What's new in adult reconstructive knee surgery, *J. Bone Joint Surg. Am.*, **94**, 182-188, DOI: 10.2106/JBJS.K.01262 [doi] (2012).

25. Ning, X. et al. Maltodextrin-based imaging probes detect bacteria in vivo with high sensitivity and specificity, *Nat. Mater.*, **10**, 602-607, DOI: nmat3074 [pii];10.1038/nmat3074 [doi] (2011).

26. Panizzi, P. et al. In vivo detection of *Staphylococcus aureus* endocarditis by targeting pathogen-specific prothrombin activation, *Nat. Med.*, **17**, 1142-1146, DOI: nm.2423 [pii];10.1038/nm.2423 [doi] (2011).

27. van, O. M. et al. Real-time *in vivo* imaging of invasive- and biomaterial-associated bacterial infections using fluorescently labelled vancomycin, *Nat. Commun.*, **4**, 2584, DOI: ncomms3584 [pii];10.1038/ncomms3584 [doi] (2013).

28. Kong, Y. et al. Imaging tuberculosis with endogenous beta-lactamase reporter enzyme fluorescence in live mice, *Proc. Natl. Acad. Sci. U. S. A*, **107**, 12239-12244, DOI: 1000643107 [pii];10.1073/pnas.1000643107 [doi] (2010).

Figure 1
Click here to download high resolution image

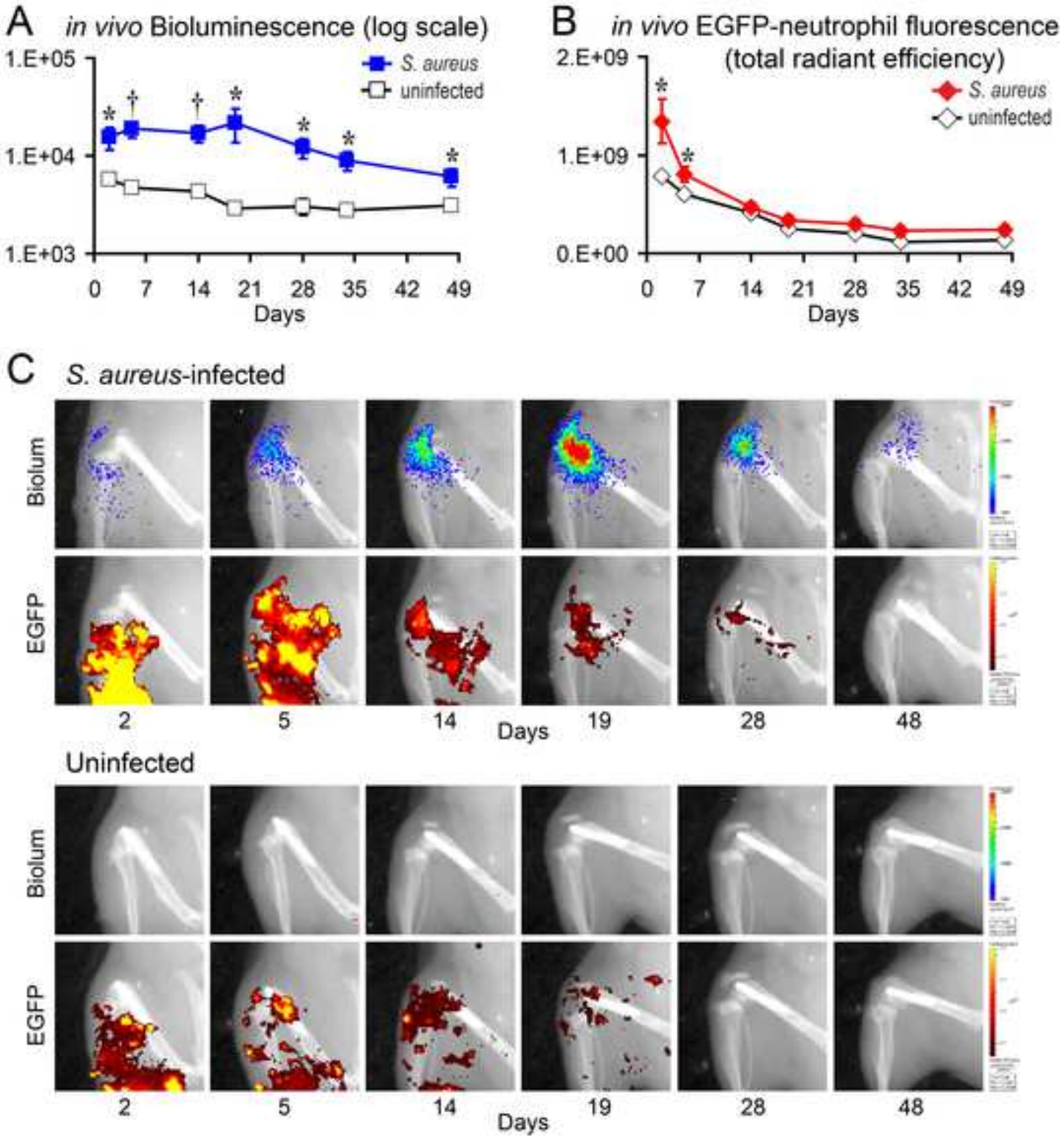

Figure 2
Click here to download high resolution image

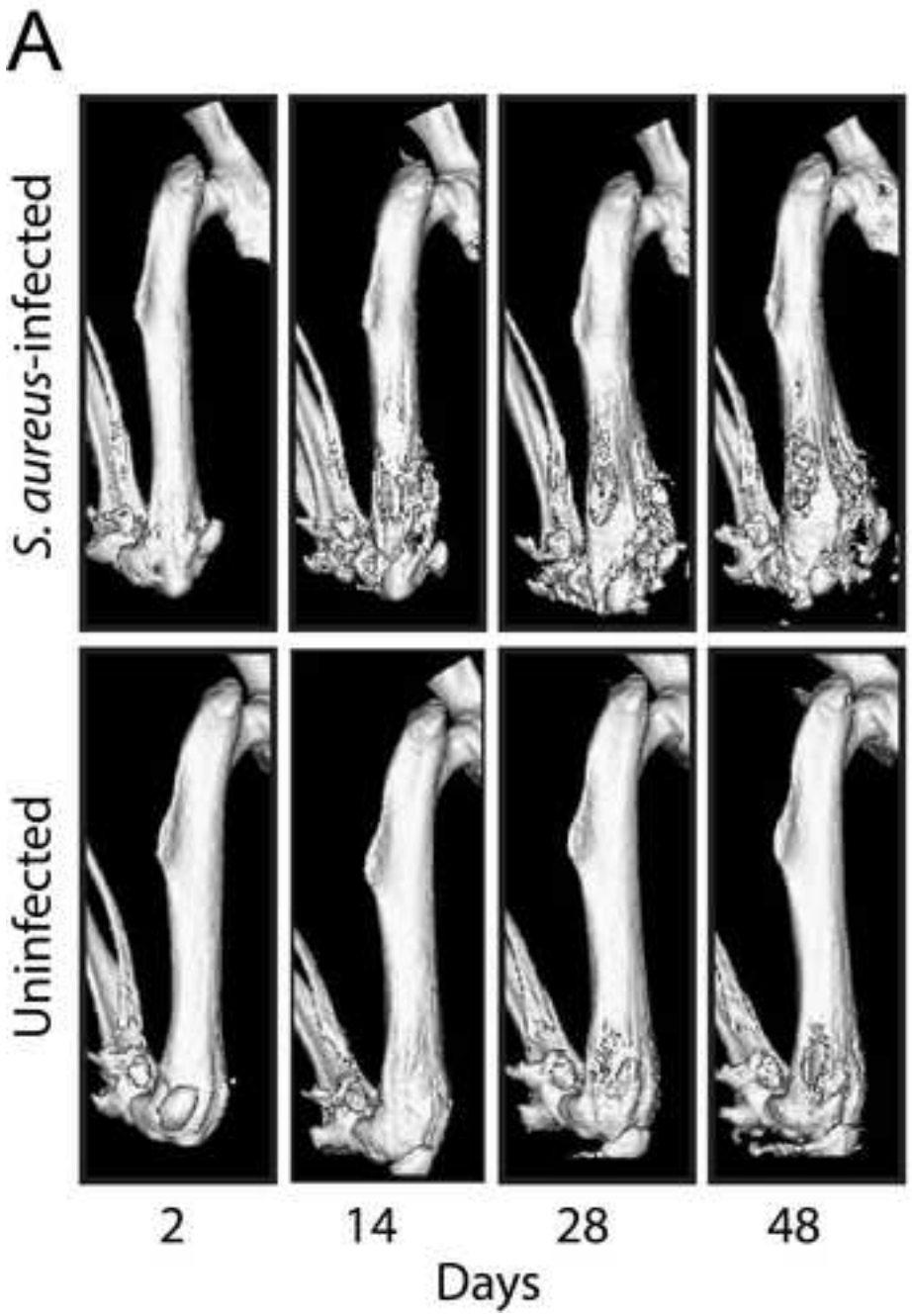

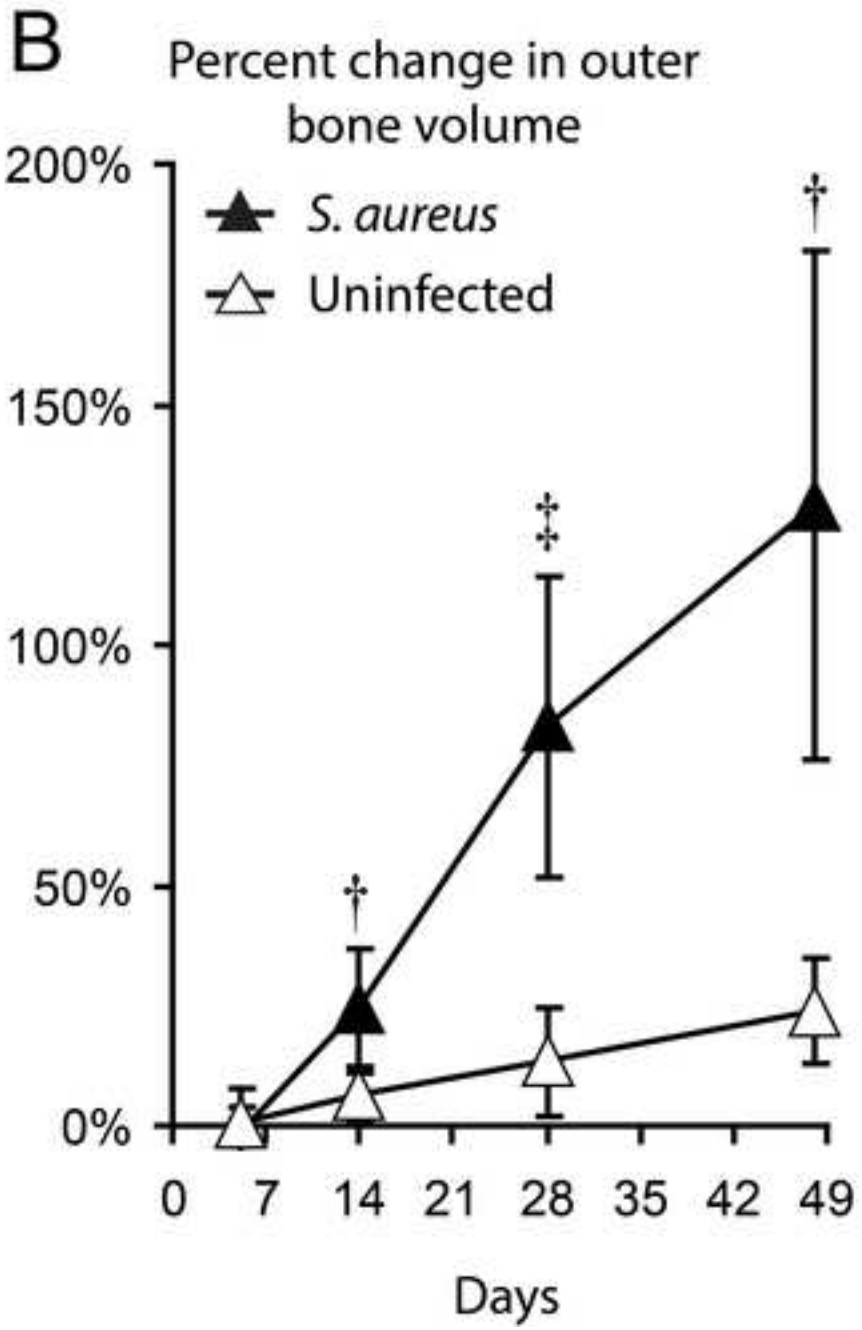

*Excel Spreadsheet- Table of Materials/Equipment

Click here to download Excel Spreadsheet- Table of Materials/Equipment: Bernthal et al JOVE_Materials.xls

Name of Material/ Equipment	Company	Catalog Number
Xen36 bioluminescent Staphylococcus aureus strain	Caliper - A PerkinElmer Company, Hopkinton, MA	
Tryptic soy broth	BD Biosciences, Franklin Lakes, NJ	211825
Bacto Soy Agar	BD Biosciences, Franklin Lakes, NJ	214010
LysEGFP knockin mouse strain		
Betadine	Purdue Products, Stamford, CT	
Kirschner-wire (titanium, 0.8 mm diameter)	Synthes, West Chester, PA	492.08
Wire Cutter - Duracut T.C.	H&H Company, Ontario, Canada	83-7002
Isoflurane	Baxter, Deerfield, IL	118718
Vicryl 5-0 sutures (P-3 Reverse cutting)	Ethicon, Summerville, NJ. Purchased through VWR International.	95056-936
Sustained-release Buprenorphine (5 ml - 1 mg/ml)	Zoopharm, Windsor, CO	
IVIS Spectrum Imaging System	Caliper - A PerkinElmer Company, Hopkinton, MA	
Quantum FX in vivo µCT system	Caliper - A PerkinElmer Company, Hopkinton, MA	
IVIS SpectrumCT Imaging System	Caliper - A PerkinElmer Company, Hopkinton, MA	
Living Image Software	Caliper - A PerkinElmer Company, Hopkinton, MA	

Comments/Description

Bioluminescent Staphylococcus aureus strain derived from ATCC 49525 (Wright), a clinical isolate from a bacteremia patient

Not commercially available. This strain contains a knockin of enhanced green fluorescence protein (EGFP) into the lysozyme M gene

analgesic

optical in vivo imaging system

µCT in vivo imaging system

combined optical and µCT in vivo imaging system

Image analysis software for in vivo optical imaging

Movie 1

Click here to download Animated Figure (video and/or .ai figure files): Movie 1.mpg

17 Sellers Street
Cambridge, MA 02139
tel. +1.617.945.9051
www.JoVE.com

ARTICLE AND VIDEO LICENSE AGREEMENT

Title of Article: Combined in vivo optical and μCT imaging to monitor infection, inflammation and bone anatomy in an orthopaedic implant infection in mice

Author(s): Nicholas M. Bernthal, Jeffrey A. Meganck, Yu Wang, Jonathan H. Shahbazian, Jared A. Niska, Kevin P. Francis and Lloyd S. Miller

Item 1 (check one box): The Author elects to have the Materials be made available (as described at http://www.jove.com/publish) via: ☐ Standard Access ☒ Open Access

Item 2 (check one box):

☒ The Author is NOT a United States government employee.

☐ The Author is a United States government employee and the Materials were prepared in the course of his or her duties as a United States government employee.

☐ The Author is a United States government employee but the Materials were NOT prepared in the course of his or her duties as a United States government employee.

ARTICLE AND VIDEO LICENSE AGREEMENT

1. Defined Terms. As used in this Article and Video License Agreement, the following terms shall have the following meanings: "**Agreement**" means this Article and Video License Agreement; "**Article**" means the article specified on the last page of this Agreement, including any associated materials such as texts, figures, tables, artwork, abstracts, or summaries contained therein; "**Author**" means the author who is a signatory to this Agreement; "**Collective Work**" means a work, such as a periodical issue, anthology or encyclopedia, in which the Materials in their entirety in unmodified form, along with a number of other contributions, constituting separate and independent works in themselves, are assembled into a collective whole; "**CRC License**" means the Creative Commons Attribution-Non Commercial-No Derivs 3.0 Unported Agreement, the terms and conditions of which can be found at: http://creativecommons.org/licenses/by-nc-nd/3.0/legalcode; "**Derivative Work**" means a work based upon the Materials or upon the Materials and other pre-existing works, such as a translation, musical arrangement, dramatization, fictionalization, motion picture version, sound recording, art reproduction, abridgment, condensation, or any other form in which the Materials may be recast, transformed, or adapted; "**Institution**" means the institution, listed on the last page of this Agreement, by which the Author was employed at the time of the creation of the Materials; "**JoVE**" means MyJove Corporation, a Massachusetts corporation and the publisher of *The Journal of Visualized Experiments;* "**Materials**" means the Article and / or the Video; "**Parties**" means the Author and JoVE; "**Video**" means any video(s) made by the Author, alone or in conjunction with any other parties, or by JoVE or its affiliates or agents, individually or in collaboration with the Author or any other parties, incorporating all or any portion of the Article, and in which the Author may or may not appear.

2. Background. The Author, who is the author of the Article, in order to ensure the dissemination and protection of the Article, desires to have the JoVE publish the Article and create and transmit videos based on the Article. In furtherance of such goals, the Parties desire to memorialize in this Agreement the respective rights of each Party in and to the Article and the Video.

3. Grant of Rights in Article. In consideration of JoVE agreeing to publish the Article, the Author hereby grants to JoVE, subject to **Sections 4** and **7** below, the exclusive, royalty-free, perpetual (for the full term of copyright in the Article, including any extensions thereto) license (a) to publish, reproduce, distribute, display and store the Article in all forms, formats and media whether now known or hereafter developed (including without limitation in print, digital and electronic form) throughout the world, (b) to translate the Article into other languages, create adaptations, summaries or extracts of the Article or other Derivative Works (including, without limitation, the Video) or Collective Works based on all or any portion of the Article and exercise all of the rights set forth in (a) above in such translations, adaptations, summaries, extracts, Derivative Works or Collective Works and (c) to license others to do any or all of the above. The foregoing rights may be exercised in all media and formats, whether now known or hereafter devised, and include the right to make such modifications as are technically necessary to exercise the rights in other media and formats. If the "Open Access" box has been checked in **Item 1** above, JoVE and the Author hereby grant to the public all such rights in the Article as provided in, but subject to all limitations and requirements set forth in, the CRC License.

4. Retention of Rights in Article. Notwithstanding the exclusive license granted to JoVE in **Section 3** above, the

Author shall, with respect to the Article, retain the non-exclusive right to use all or part of the Article for the non-commercial purpose of giving lectures, presentations or teaching classes, and to post a copy of the Article on the Institution's website or the Author's personal website, in each case provided that a link to the Article on the JoVE website is provided and notice of JoVE's copyright in the Article is included. All non-copyright intellectual property rights in and to the Article, such as patent rights, shall remain with the Author.

5. Grant of Rights in Video – Standard Access. This **Section 5** applies if the "Standard Access" box has been checked in **Item 1** above or if no box has been checked in **Item 1** above. In consideration of JoVE agreeing to produce, display or otherwise assist with the Video, the Author hereby acknowledges and agrees that, Subject to **Section 7** below, JoVE is and shall be the sole and exclusive owner of all rights of any nature, including, without limitation, all copyrights, in and to the Video. To the extent that, by law, the Author is deemed, now or at any time in the future, to have any rights of any nature in or to the Video, the Author hereby disclaims all such rights and transfers all such rights to JoVE.

6. Grant of Rights in Video – Open Access. This **Section 6** applies only if the "Open Access" box has been checked in **Item 1** above. In consideration of JoVE agreeing to produce, display or otherwise assist with the Video, the Author hereby grants to JoVE, subject to **Section 7** below, the exclusive, royalty-free, perpetual (for the full term of copyright in the Article, including any extensions thereto) license (a) to publish, reproduce, distribute, display and store the Video in all forms, formats and media whether now known or hereafter developed (including without limitation in print, digital and electronic form) throughout the world, (b) to translate the Video into other languages, create adaptations, summaries or extracts of the Video or other Derivative Works or Collective Works based on all or any portion of the Video and exercise all of the rights set forth in (a) above in such translations, adaptations, summaries, extracts, Derivative Works or Collective Works and (c) to license others to do any or all of the above. The foregoing rights may be exercised in all media and formats, whether now known or hereafter devised, and include the right to make such modifications as are technically necessary to exercise the rights in other media and formats. For any Video to which this Section 6 is applicable, JoVE and the Author hereby grant to the public all such rights in the Video as provided in, but subject to all limitations and requirements set forth in, the CRC License.

7. Government Employees. If the Author is a United States government employee and the Article was prepared in the course of his or her duties as a United States government employee, as indicated in **Item 2** above, and any of the licenses or grants granted by the Author hereunder exceed the scope of the 17 U.S.C. 403, then the rights granted hereunder shall be limited to the maximum rights permitted under such statute. In such case, all provisions contained herein that are not in conflict with such statute shall remain in full force and effect, and all provisions contained herein that do so conflict shall be deemed to be amended so as to provide to JoVE the maximum rights permissible within such statute.

8. Likeness, Privacy, Personality. The Author hereby grants JoVE the right to use the Author's name, voice, likeness, picture, photograph, image, biography and performance in any way, commercial or otherwise, in connection with the Materials and the sale, promotion and distribution thereof. The Author hereby waives any and all rights he or she may have, relating to his or her appearance in the Video or otherwise relating to the Materials, under all applicable privacy, likeness, personality or similar laws.

9. Author Warranties. The Author represents and warrants that the Article is original, that it has not been published, that the copyright interest is owned by the Author (or, if more than one author is listed at the beginning of this Agreement, by such authors collectively) and has not been assigned, licensed, or otherwise transferred to any other party. The Author represents and warrants that the author(s) listed at the top of this Agreement are the only authors of the Materials. If more than one author is listed at the top of this Agreement and if any such author has not entered into a separate Article and Video License Agreement with JoVE relating to the Materials, the Author represents and warrants that the Author has been authorized by each of the other such authors to execute this Agreement on his or her behalf and to bind him or her with respect to the terms of this Agreement as if each of them had been a party hereto as an Author. The Author warrants that the use, reproduction, distribution, public or private performance or display, and/or modification of all or any portion of the Materials does not and will not violate, infringe and/or misappropriate the patent, trademark, intellectual property or other rights of any third party. The Author represents and warrants that it has and will continue to comply with all government, institutional and other regulations, including, without limitation all institutional, laboratory, hospital, ethical, human and animal treatment, privacy, and all other rules, regulations, laws, procedures or guidelines, applicable to the Materials, and that all research involving human and animal subjects has been approved by the Author's relevant institutional review board.

10. JoVE Discretion. If the Author requests the assistance of JoVE in producing the Video in the Author's facility, the Author shall ensure that the presence of JoVE employees, agents or independent contractors is in accordance with the relevant regulations of the Author's institution. If more than one author is listed at the beginning of this Agreement, JoVE may, in its sole discretion, elect not take any action with respect to the Article until such time as it has received complete, executed Article and Video License Agreements from each such author. JoVE reserves the right, in its absolute and sole discretion and without giving any reason therefore, to accept or decline any work submitted to JoVE. JoVE and its employees, agents and independent contractors shall have full, unfettered access to the facilities of the Author or of the Author's institution as necessary to make the Video, whether actually published or not. JoVE has sole discretion as to the method of making and publishing the Materials, including,

17 Sellers Street
Cambridge, MA 02139
tel. +1.617.945.9051
www.JoVE.com

ARTICLE AND VIDEO LICENSE AGREEMENT

without limitation, to all decisions regarding editing, lighting, filming, timing of publication, if any, length, quality, content and the like.

11. Indemnification. The Author agrees to indemnify JoVE and/or its successors and assigns from and against any and all claims, costs, and expenses, including attorney's fees, arising out of any breach of any warranty or other representations contained herein. The Author further agrees to indemnify and hold harmless JoVE from and against any and all claims, costs, and expenses, including attorney's fees, resulting from the breach by the Author of any representation or warranty contained herein or from allegations or instances of violation of intellectual property rights, damage to the Author's or the Author's institution's facilities, fraud, libel, defamation, research, equipment, experiments, property damage, personal injury, violations of institutional, laboratory, hospital, ethical, human and animal treatment, privacy or other rules, regulations, laws, procedures or guidelines, liabilities and other losses or damages related in any way to the submission of work to JoVE, making of videos by JoVE, or publication in *JoVE* or elsewhere by JoVE. The Author shall be responsible for, and shall hold JoVE harmless from, damages caused by lack of sterilization, lack of cleanliness or by contamination due to the making of a video by JoVE its employees, agents or independent contractors. All sterilization, cleanliness or decontamination procedures shall be solely the responsibility of the Author and shall be undertaken at the Author's expense. All indemnifications provided herein shall include JoVE's attorney's fees and costs related to said losses or damages. Such indemnification and holding harmless shall include such losses or damages incurred by, or in connection with, acts or omissions of JoVE, its employees, agents or independent contractors.

12. Fees. To cover the cost incurred for publication, JoVE must receive payment before production and publication the Materials. Payment is due in 21 days of invoice. Should the Materials not be published due to an editorial or production decision, these funds will be returned to the Author. Withdrawal by the Author of any submitted Materials after final peer review approval will result in a US$1,200 fee to cover pre-production expenses incurred by JoVE. If payment is not received by the completion of filming, production and publication of the Materials will be suspended until payment is received.

13. Transfer, Governing Law. This Agreement may be assigned by JoVE and shall inure to the benefits of any of JoVE's successors and assignees. This Agreement shall be governed and construed by the internal laws of the Commonwealth of Massachusetts without giving effect to any conflict of law provision thereunder. This Agreement may be executed in counterparts, each of which shall be deemed an original, but all of which together shall be deemed to me one and the same agreement. A signed copy of this Agreement delivered by facsimile, e-mail or other means of electronic transmission shall be deemed to have the same legal effect as delivery of an original signed copy of this Agreement.

A signed copy of this document must be sent with all new submissions. Only one Agreement required per submission.

AUTHOR:

Name: Lloyd S. Miller

Department: Department of Dermatology

Institution: Johns Hopkins University School of Medicine

Article Title: Combined in vivo optical and μCT imaging to monitor infection, inflammation and bone anatomy in an orthopaedic implant infection in mice

Signature: 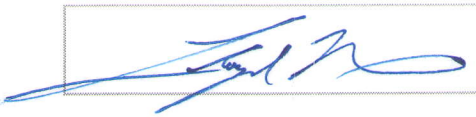 Date: 8/30/13

Please submit a signed and dated copy of this license by one of the following three methods:

1) Upload a scanned copy as a PDF to the *JoVE* submission site upon manuscript submission (preferred);
2) Fax the document to +1.866.381.2236; or
3) Mail the document to *JoVE* / Attn: *JoVE* Editorial / 17 Sellers St / Cambridge, MA 02139

For questions, please email editorial@jove.com or call +1.617.945.9051.

MS # (internal use):

Rebuttal Comments

Click here to download Rebuttal Comments: Bernthal et al Rebuttal Letter 12-29-2013_FINAL.pdf

Johns Hopkins Department of Dermatology
Cancer Research Building II, Suites 209 & 210
1550 Orleans Street
Baltimore, MD 21231
410-955-8662 T
410-955-8645 F

JOHNS HOPKINS
MEDICINE

December 29, 2013

Dear Editors,

Thank you for the review of our manuscript for JoVE. Below is a list of the revisions that were made in response to the comments by the Editors and Reviewer 1 and 2, point-by-point:

EDITORIAL COMMENTS:

1) All of your previous revisions have been incorporated into the most recent version of the manuscript. Please download this version of the Microsoft word document from the "file inventory" to use for any subsequent changes.

RESPONSE: This was done as suggested.

2) Please disregard the comment below if all of your figures are original.
If you are re-using figures from a previous publication, you must obtain explicit permission to re-use the figure from the previous publisher (this can be in the form of a letter from an editor or a link to the editorial policies that allows you to re-publish the figure). Please upload the text of the re-print permission (may be copied and pasted from an email/website) as a Word document to the Editorial Manager site in the "Supplemental files (as requested by JoVE)" section. Please also cite the figure appropriately in the figure legend, i.e. "This figure has been modified from [citation]."

RESPONSE: All figures will be original figures.

3) Please take this opportunity to thoroughly proofread your manuscript to ensure that there are no spelling or grammar issues. Your JoVE editor will not copy-edit your manuscript and any errors in your submitted revision may be present in the published version.

RESPONSE: This was done as suggested.

4)"2.7) Inoculate 2 µL of $1x10^3$ CFU of bioluminescent *S. aureus* Xen36 into the knee joint space." This process is not described in enough detail. How are the bacteria injected into the joint space?

RESPONSE: The new step 2.9 (Page 5, Line 213) was changed to:
"Using a micropipette, pipette 2 µL of $1x10^3$ CFU of bioluminescent *S. aureus* Xen36 onto the tip of the implant within the knee joint space."

5) Should the mouse in 4.1 be anesthetized?

RESPONSE: Step 4.1 (Page 5, line 282) was changed to "Place anesthetized LysEGFP mice into an imaging chamber."

5) Step 2.9 refers to something that should be done prior to surgery, but is presented after the surgery is complete. Please present action in chronological order

RESPONSE: This step was moved to step 2.2 (Page 5, lines 187-189) and the steps were reordered so that they are in chronological order.

6) Some issues regarding Notes:

-The Note before 2.1 contains protocol steps that use the wrong verb tense.

RESPONSE: The Note before 2.1 (Page 14, lines 173-182) was changed to the present verb tense.

-"2.5) ...into the intramedullary canal using". This sentence fragment should be finished with "Titanium K-wires." and not left with that information only in the "note".

RESPONSE: The word "using" was a mistake and was deleted. This sentence (Page 5, Lines 205-207) was revised to end with "…into the intramedullary canal."

-Note in step 2.9 contains information which should be included as a step at the appropriate time. "At the end of the experiments, all animals were euthanized ..."

RESPONSE: This information is now included in step 2.11 (page 5, Lines 225-228).

-Note in 5.2.2 does not appear to be optional or additional information and should be included as part of the protocol in the appropriate location.

RESPONSE: Notes have been removed and worked into the steps 5.2/5.2.1/5.2.2 in the appropriate locations. The steps have been reworded slightly to better reflect software selections and accommodate the smooth inclusion of these notes into the text.

REVIEWER #1 COMMENTS:

Minor Concerns:
Four other references should be included referring to probe development:
Ning, X. et al. Maltodextrin-based imaging probes detect bacteria in vivo with high sensitivity and specificity. Nat. Mater. 10, 602-607 (2011).

Panizzi, P. et al. In vivo detection of Staphylococcus aureus endocarditis by targeting pathogen-specific prothrombin activation. Nat. Med. 17, 1142-1146 (2011).

Kong, Y. et al. Imaging tuberculosis with endogenous beta-lactamase reporter enzyme fluorescence in live mice. Proc. Natl Acad. Sci. USA 107, 12239-12244 (2010).

van Oosten, M. et al. Real-time in vivo imaging of invasive- and biomaterial-associated bacterial infections using fluorescently labelled vancomycin. Nat. Commun. 4:2584 doi: 10.1038/ncomms3584 (2013)

RESPONSE: As suggested, these 4 references have been added to the statement referring to probe development (Page 12, Lines 533-536).

REVIEWER #2 COMMENTS:

Major Concerns:

1) One specific conclusion that is not supported by the data is correlation between bioluminescence signal and the bioburden (CFU). This information is in particular important, as authors indicate the strain of bacteria (Xen29) used to generate current data will be replaced with a different *S. aureus* strain (Xen36). Authors need to provide the survival and growth rate of Xen36 *in vivo* and the correlation of bioluminescence signal to CFU.

RESPONSE: In 3 of our prior published manuscripts, we have provided information about the survival and growth rate of Xen36 *in vivo* (Pribaz, J et al. 2012 *J. Orthop. Res* 30:335–340[19]) and we enumerated CFU from the joint/bone tissue and implants and the numbers of CFU closely approximate the bioluminescent signals taken at the same time points (Niska, JA, et al. 2012 *Antimicrob Agents Chemother* 56: 2590-2597 [17] and Niska, JA, et al. 2013. *Antimicrob Agents Chemother* 57: 5080-5086[18]). To include this information in the current manuscript, the following sentence was added to the REPRESENTATIVE RESULTS section "*In vivo* bioluminescent and fluorescent imaging" in the second to last sentence (Page 10, Lines 435-437):

"Our previous work demonstrated that the *in vivo* bioluminescent signals closely approximated the numbers of *ex vivo* CFU isolated from the joint/bone tissue and adherent to the implants [17, 18]."

2) Important control group appears to be missing. Please show the survival / persistence of test organism with no foreign body implant in the knee.

RESPONSE: Although we appreciate this suggestion to add this control group, a control group without an implant would model *S. aureus* septic arthritis rather than an orthopaedic implant *S. aureus* infection. Since the purpose of this manuscript is to provide the methods to model an orthopaedic implant infection, this experimental group is not indicated for this study.

3.1) Fig . 1. Bioluminescence signal appears to increase over time, reaching a peak around day 19. However, the neutrophil signal seems to disappear rapidly. Do the authors have any explanation as to why there is no recruitment of neutrophils to the site of infection with the progression of infection?
3.2) What is the average life span of activated and non-activated neutrophils in this mouse strain LysEGFP?
3.3) What is the repeated exposure X-ray irradiation on neutrophil production?
PLEASE SEE THE SPECIFIC RESPONSES TO EACH OF THESE QUESTIONS, FOLLOWED BY REVISED TEXT IN THE MANUSCRIPT, BELOW:

3.1) RESPONSE: In our previous work, we compared 4 different bioluminescent *S. aureus* strains (ALC2906, Xen29, Xen36 and Xen40) in LysEGFP mice using this same orthopaedic implant infection model without any X-ray irradiation (Pribaz, J et al. 2012 J. Orthop. Res 30:335–340[19]). We observed some differences in EGFP-neutrophil signals among the different *S. aureus* strains, suggesting different strains induce varying degrees neutrophilic inflammation. However, all of the neutrophil EGFP signals decreased to background levels by 14-21 days after infection and remained at background levels through day 42 when the experiment was arbitrarily terminated. Although we do not know exactly why the neutrophil signals decreased, it is likely that the infection over time becomes more chronic, and as this occurs, perhaps the immune response is no longer dominated by neutrophil infiltration as with other chronic infections. This subject is area of ongoing investigation in our lab and is beyond the purpose of this manuscript, which is focused on presenting the methods of using noninvasive *in vivo* imaging to monitor the infection and neutrophil infiltration in a mouse model of orthopaedic implant infection.

3.2) RESPONSE: During a *S. aureus* skin wound infection in LysEGFP mice, we found that neutrophils survived 3-fold longer (4.96 ± 0.38 days) in *S. aureus*-infected wounds compared with uninfected wounds (1.58 ± 0.31 days) (Kim, M-H, et al. 2011. *Blood* 117: 3343-3352[23]). The increased life-span is likely due to survival signals such as TLR2 and PGE2 as we previously described (Granick, JL, et al. 2013. *Blood* 122:1770-1778). In the *S. aureus* wound infection model, we identified that neutrophil infiltration involved 3 main mechanisms: (1) robust neutrophil recruitment from the circulation, (2) prolonged neutrophil survival at the site of infection and (3) the homing of KIT+ progenitor cells to the abscess, where they locally give rise to mature neutrophils (Kim, M-H, et al. 2011. *Blood* 117: 3343-3352[23]). From these prior studies, we expect that similar mechanisms will contribute to neutrophil infiltration to the site of the orthopaedic implant *S. aureus* infection and the neutrophils will survive longer in infected mice compared with uninfected mice.

3.3) RESPONSE: We did not measure the effect of X-ray irradiation on neutrophil production but the X-ray irradiation likely had minimal impact on neutrophil production or the kinetics of the neutrophil recruitment to the site of infection because neutrophil fluorescence in this model had the same kinetics in non-irradiated mice (Pribaz, J et al. 2012 J. Orthop. Res 30:335–340[19]) as irradiated mice (Niska, JA, et al. 2012. *PLOS ONE* 7(10): e47397[16]).

To include the responses to major concern 3 (3.1, 3.2, 3.3) in the manuscript, the following text has been added to the Discussion page 11, lines 504-516:

"One interesting finding that should be pointed out is that we observed that the EGFP-neutrophil fluorescent signals decreased to background levels by 14-21 days and remained at background levels for the duration of the experiment despite the presence of bioluminescent bacteria. It is unlikely that the X-ray irradiation impacted neutrophil survival as we observed similar kinetics of the neutrophil signals in non-irradiated mice[19]. In our previous work involving a model of S. aureus infected wounds, neutrophil infiltration involved a combination of robust neutrophil recruitment from the circulation, prolonged neutrophil survival at the site of infection and the homing of KIT+ progenitor cells to the abscess, where they locally give rise to mature neutrophils[23]. It is likely that similar processes contributed to neutrophil infiltration in the orthopaedic implant S. aureus infection model. Although it is unknown why the neutrophil signals decreased in the orthopaedic infection model, it could be that the immune response changed over time as this infection progressed from an acute to chronic infection and this is a subject of future investigation."

4) Page 11 line 485. Although stated to be the case by the authors, there is no monitoring of bacterial burden in this study. In order to demonstrate this, it is essential to establish in vivo correlation between bioluminescence signal and CFU for Xen29 and Xen36.

RESPONSE: Please see the above response to major concern #1.

Minor Concerns:
1) Page 4, line145. Please confirm if lux operon is integrated into bacterial chromosome or plasmid.

RESPONSE: This sentence was changed to read: "Note: *S. aureus* Xen36[21] is a genetically engineered *S. aureus* strain that contains a modified *lux* operon derived from *Photorhabdus luminescens*, which is integrated into a stable native plasmid found in this bacterial strain."

2) Page 4. No method given for cultivation and preparation of bacterial inocula.

RESPONSE: We have provided the method for cultivation and preparation of the bacterial inocula in the Protocol steps 1.1 to 1.7 (page 4, lines 141-163).

3) Page 5. Please indicate whether the animals in control group (uninfected) were subjected to the same surgical procedure as test group.

RESPONSE: We thank Reviewer 2 for pointing this out. The following Note was added to step 2.7:
"Note: In control uninfected mice, 2 µL of sterile saline is added without any bacteria."

4) What is the limit of detection of test organism and neutrophils in this model?
RESPONSE: Based on our previous work we can accurately detect between $1x10^2$ and $1x10^3$ bacteria using *in vivo* bioluminescent imaging. We have not measured the limit of detection of neutrophils. To include this in the manuscript, the following sentence as added to the Figure 1 Legend, page 11, lines 470-471:
"The limit of detection of the bacterial burden using *in vivo* bioluminescent imaging is between $1x10^2$ and $1x10^3$ CFU."

5) Page 5, line 225 (3.1). Were the images acquired from dorsal or ventral side of animal?

RESPONSE: Images were acquired from the ventral side. The following was added to step 3.1 (Page 6, lines 233-234):
"3.1) Anesthetize LysEGFP mice (e.g., 2% inhalation isoflurane) and place them with ventral side up into an imaging chamber."

6) Page 5, line 228. (3.2). Which series of IVIS imaging system is used in the study?

RESPONSE: Page 6, line 237, in step 3.2, the following IVIS system was used as is mentioned: "3.2) Perform *in vivo* bioluminescent imaging using the IVIS Spectrum optical whole animal *in vivo* imaging system (PerkinElmer, Inc.)."

7) Page 6, line 233. (3.2). How long were the animals imaged per session?

RESPONSE: The following Note has been added to steps 3.2 and 3.3 (Page 6, lines 242 and 247, respectively):
3.2) "Note: For *in vivo* bioluminescent imaging, mice are typically imaged between 1 to 5 minutes."
3.3) "Note: For *in vivo* fluorescent imaging, mice are typically imaged between 0.5 seconds."

Thank you for the review of our manuscript. We hope that we adequately addressed all of the concerns of the reviewers.

Sincerely,

Lloyd S. Miller, M.D., Ph.D.
Associate Professor
Department of Dermatology
Department of Medicine, Division of Infectious Diseases
Department of Orthopaedic Surgery